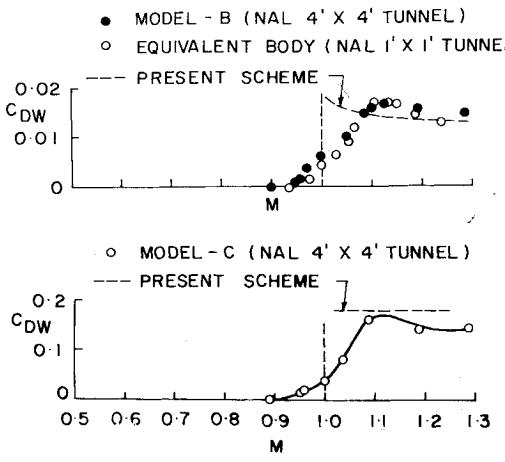

Fig. 2 Comparison of wave drag values by the present scheme with the experimental results of NAL-Model B and Model C.

Discussion of Results

The results obtained by the present scheme for these examples are compared with those by the schemes of Eminton[3,4] and Shanbhag and Narasimha[5,6] (see Table 1).

In Table 1 the value of the double integral (1) and the contribution T from the terms of Eq. (1a) are shown separately. In the scheme due to Eminton, T is exactly zero in all case since $S'(1)$ is forced to be zero. In Example A, $S'(1)=0$ exactly but $T\neq 0$ by the present scheme, as well as by that of Shanbhag and Narasimha due to numerical differentiation errors. However, as can be seen from Table 1 the contribution from T has a compensating effect on the final value in the present method. Furthermore, taking the contribution of the extra terms seems to reduce the sensitivity of the final value to the numerical interpolation schemes used in obtaining the derivative values.

In the Examples B and C, $S'(1)\neq 0$ and therefore $T\neq 0$, except in the case of Eminton's scheme as metnioned earlier. The comparison with the experimental results (Figs. 2) seems to indicate, that in the present scheme the contribution from T has again a desirable effect on the drag value. Furthermore, to some extent, the sensitivity to interpolating schemes is again found to be reduced by taking into account the contribution of T. This does not seem to be the case with the scheme of Shanbhag and Narasimha.

It may be noted here that for the case of Example B the double integral alone by the scheme of Shanbhag and Narasimha is closer to the maximum of the experimentally observed wave drag in the transonic regime. Consideration of the contribution due to T gives here a considerably lower value than the experimental values. In the case of Example C where discontinuities exist in the $S'(\xi)$, numerical value of $S''(\xi)$ around these discontinuities are not realistic and these result in unrealistic values of wave drag by the scheme of Shanbhag and Narasimha, therefore, these drag values have been omitted from Table 1.

The comparison of the present results with the experimental results shown in Fig. 2 shows that, apart from the reliability of the present scheme in the transonic regime, the agreement is very good for $M>1.20$. This shows that the present scheme would be quite useful in conjunction with supersonic area rule. Computation times on the IBM 360-44 machine were small and comparable for all the methods tried here.

In conclusion, the present simple method, requiring, as it does, only the first-derivative values of the area distribution, seems to be more reliable than the rest of the methods known in literature for evaluating the transonic wave drag.

References

[1]Liepmann, H.W. and Roshko, A., *Elements of Gas Dynamics*, Wiley, New York, 1960, pp. 238-239.

[2]Lighthill, M.J., "Supersonic Flow Past Slender Bodies of Revolution, the Slope of Whose Meridian Section is Discontinuous," *Quarterly Journal of Mechanics and Applied Mathematics*, Vol. 1, 1948, pp. 90-102.

[3]Eminton, E., "On the Minimisation and Numerical Evaluation of Wave Drag," Royal Aeronautical Establishment, Farnborough, England, RAE Rept. Aero 2564, 1955.

[4]Shanbhag, V.V. and Narasimha, R., "Numerical Evaluation of the Transonic Wave Drag Integral," *International Journal for Numerical Methods in Engineering*, Vol. 2, 1970, pp. 277-282.

[5]Shanbhag, V.V. and Narasimha, R., "On the Spline Approximation for Integrals with a Logarithmic Kernel," National Aeronautics Laboratory, Bangalore, India, NAL Tech. Note, TN-27, May 1970.

[6]James, R.M. and Panico, V.D., "Evaluation of Drag Integral Using the Cubic Splines," *Journal of Aircraft*, Vol. 11, Aug. 1974, pp. 494-496.

[7]Butler S.F.J., "Aircraft Drag Prediction for Project Appraisal and Performance Estimation," AGARD-CP-124, 1973.

Static Aeroelastic Twist Effects on Helicopter Rotor-Induced Velocity

K.S. Nagaraja* and G. Alvin Pierce†
Georgia Institute of Technology, Atlanta, Georgia

Introduction

UNLIKE fixed-wing aircraft, the unsteady aerodynamic flowfield associated with a helicopter rotor, in hover or vertical flight, at low inflow conditions is indeed complicated. This is mainly due to the close proximity of the unsteady wake vortices beneath the rotor. In such a case, the use of fixed-wing unsteady aerodynamic theory in the flutter and dynamic response analyses is highly questionable. Unsteady aerodynamic theories have been developed[1-3] to account for the presence of wake beneath the rotor. To compute the unsteady airloads using these theories, the required wake spacing, h, beneath the rotor, is generally computed by using the combined blade element-momentum theory,[4] assuming the blade to be rigid. However, the rotor blade is flexible, both in torsion and bending, and, hence, there will be a change in the mean induced velocity distribution due to the static elastic twist of the blade. For a more realistic wake spacing, the effect of static elastic twist should be considered. In this Note, an approximate analytical treatment is given to determine the static elastic twist and the mean inflow velocity distribution. This inflow velocity can then be used to compute the wake spacing required for determining the unsteady airloads.

Analysis

Consider an elastic uniform untwisted blade in hover or vertical flight V, fixed at a distance a outboard from the axis of rotation and set at a pitch angle α_r. The actual blade is elastic both in torsion and bending, and hence it deforms under steady aerodynamic loads. However, in the present analysis, the edgewise bending stiffness is assumed to be large. Also, the effect of flapwise bending deformations on elastic twist θ is small in practice and hence one need only consider the torsional equilibrium equation in the analysis. The equilibrium equation in torsion[5] is

$$-(\mathrm{d}/\mathrm{d}r)\{[1+(Tk_A^2/GJ)](\mathrm{d}\theta/\mathrm{d}r)\}+K_J\theta=(M(r)/GJ)-K_2 \quad (1)$$

Received Feb. 23, 1976; revision received May 26, 1976.

Index categories: Rotary Wing Aerodynamics; Nonsteady Aerodynamics; Aeroelasticity and Hydroelasticity.

*Graduate Research Assistant. Presently Dynamics Engineer with Beech Aircraft Corporation, Wichita, Kansas.

†Professor, School of Aerospace Engineering. Member AIAA.

For a uniform blade the polar radius of gyration k_A, the torsional stiffness GJ and parameters K_1 and K_2 are constant along the length. However, the centrifugal tension T is a function of radial station r and is given by $\int_r^R \Omega^2 mr dr$ for a rotational frequency Ω, a mass per unit length m and radius R of the blade. $M(r)$ is the torque per unit span at station r about the elastic axis and can be obtained by considering the aerodynamic and gravity forces on a two-dimensional blade element of the rotor blade. It is given by

$$M(r) = cc_\ell q e_{AC} \cos(\alpha_r + \theta - \phi) + c^2 c_{m_{AC}} q - Nmge \cos(\alpha_r + \theta) \tag{2}$$

where

$$q = \tfrac{1}{2}\rho_\infty [(\Omega r)^2 + (V+v)^2]$$

$$c_\ell = \bar{a} \sin(\alpha_r + \theta - \phi)$$

$$\phi = \tan^{-1}(V+v)/\Omega r \text{ (inflow angle)}$$

and e_{AC} is the distance between aerodynamic center and elastic axis, e is the distance between center of gravity and elastic axis, and N is the load factor normal to the rotor plane. Unlike in fixed-wing aircraft, the induced velocity v and inflow angle ϕ in the case of a helicopter rotor is quite large and cannot be neglected in the analysis.

Considering the elastic twist θ of the blade, an approximate representation of the induced velocity at a spanwise station r is obtained using the combined blade element-momentum theory[4] and is given by

$$\frac{v}{\Omega R} = -\left|\left[\frac{V_a}{2} + \frac{\bar{a}\sigma}{16}\cos(\alpha_r+\theta)\right] + \left\{\left[\frac{V_a}{2} + \frac{\bar{a}\sigma}{16}\cos(\alpha_r+\theta)\right]^2 + \frac{\bar{a}\sigma}{8}\left[\frac{r}{R}\sin(\alpha_r+\theta) - V_a\cos(\alpha_r+\theta)\right]\right\}^{1/2}\right| \tag{3}$$

where $V_a = V/\Omega R, \sigma = c/\pi R$ and $\bar{a}$ is the lift curve slope of the blade element. The boundary conditions for the rotor are

$$\theta = 0 \quad \text{at} \quad r = a$$
$$d\theta/dr = 0 \quad \text{at} \quad r = R \tag{4}$$

Equations (1) and (3) are coupled nonlinear equations to be solved in conjunction with the boundary conditions of Eq. (4). Linearization of the equations is not possible because of the presence of θ under the radical in Eq. (3) and v, ϕ in Eq. (2). Hence Eqs. (1) and (3) are solved numerically to satisfy the boundary conditions in Eq. (4). However, deliberately assuming that v and ϕ are small compared to v and $\alpha_r + \theta$, respectively, Eq. (1) can be linearized, and this uncouples Eqs. (1) and (3).

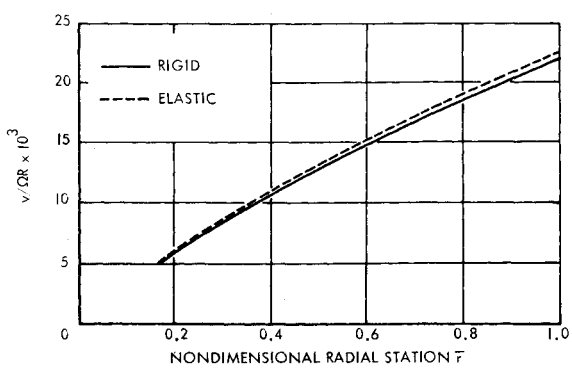

Fig. 1 Elastic effect on the nondimensional induced velocity

Numerical Procedure

The coupled nonlinear equations are solved numerically using a standard Runge-Kutta method for initial-value problems.[6] The procedure here is to treat the solution of the boundary-value problem as the iterative solution of an initial-value problem. Assuming a certain value for $d\theta/dr$ at the root $r = a$ and using the known initial condition at the root, the Runge-Kutta method is used to solve numerically Eq. (1) for the value of $d\theta/dr$ at the tip. This value is compared with the actual boundary condition at the tip. If it is different, another value of $d\theta/dr$ is assumed at the root, and the procedure is repeated. For some value of $d\theta/dr$ at the root, the boundary condition at the tip is satisfied. The nonlinearity associated with the differential equation is weak and the unknown functions are smooth; hence the above procedure was found to be satisfactory.

Results and Discussion

Properties for an elastic model blade used in the experimental investigation[7] are considered for the numerical results. Figures 1 and 2 show the effect of elastic twist of the blade on inflow distribution at rotor tip speeds of 125.7 and 418.9 ft/sec. Aerodynamic tip losses were not considered in the analysis. The effect of elastic twist is to increase the inflow velocity as compared to a rigid-blade assumption. Also, this effect is small at lower speeds as expected. The increase in inflow velocity increases the wake spacing required for the flutter or dynamic response analysis of the elastic hovering blade. Hence, the flutter speed[8] computed by accounting for the effect of elastic twist on wake spacing is generally higher than otherwise obtained.

The effect of rotor-tip speed on the elastic twist at the tip for different pitch angles α_r is shown in Fig. 3. It can be observed that the elastic twist increases rapidly at higher speeds and even more at higher pitch angles. This is an indication of approaching divergence speed, at which the blade is statically unstable.

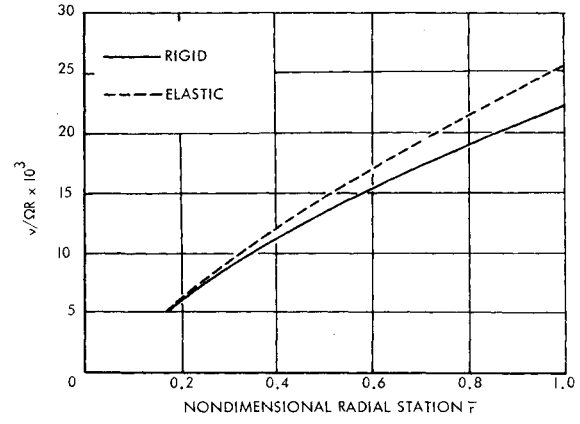

Fig. 2 Ela effect on the nondimensional induced veloci distribution , $V = 0$, $\alpha_r = 2°$, and tip speed = 418.9 ft/sec.

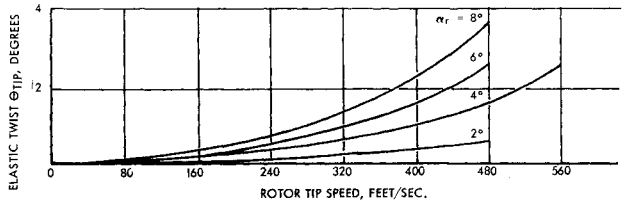

Fig. 3 Effect of rotor tip speed on the elastic twist at the tip, for ferent rigid pitch angles with $V = 0$.

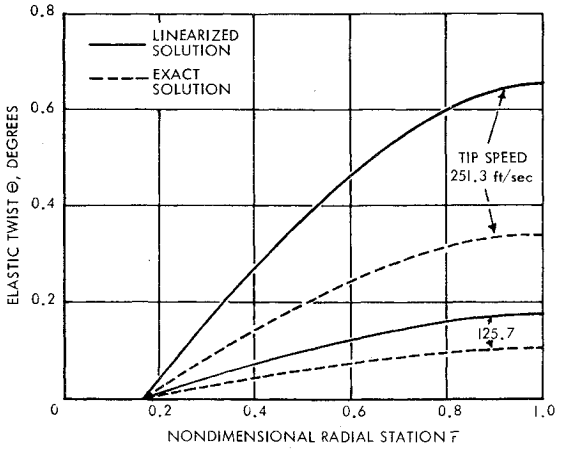

Fig. 4 Comparison of the linearized solution with the exact solution for elastic twist (with $V=0$, $\alpha_r=4°$).

Results obtained by solving the linearized form of Eq. (1) are shown in Fig. 4. The solution of the linearized equation yield higher elastic-twist distribution than the exact solution from Eqs. (1) and (3). Consequently, the inflow velocity distribution is increased and is greater than the corresponding exact solution as discussed previously.

References

[1] Loewy, R. G., "A Two Dimensional Approximation to the Unsteady Aerodynamics of Rotary Wing," *Journal of the Aerospace Sciences*, Vol. 24, Feb. 1957, pp. 81-92.

[2] Jones, W. P. and Rao, B. M., "Compressibility Effects on Oscillating Rotor Blades in Hovering Flight," *AIAA Journal*, Vol. 8, Feb. 1970, pp. 321-329.

[3] Hammond, C. E. and Pierce, G. A., "A Compressible Unsteady Aerodynamic Theory for Helicopter Rotors," AGARD CPNo. 111: *Aerodynamics of Rotary Wings*, pp. 13-1 to 13-15, Feb. 1973.

[4] Gessow, A. and Myers, G. C., Jr., *Aerodynamics of the Helicopter*, Frederick Ungar Publishing Co., New York, 1967, pp. 66-69.

[5] Houbolt, J. C. and Brooks, G. W., "Differential Equations of Motion for Combined Flapwise Bending, Chordwise Bending, and Torsion of Twisted Nonuniform Rotor Blades," NACA Technical Report 1346, 1958.

[6] Carnaham, B., Luther, H. A., and Wilkes, J. O., *Applied Numerical Methods*, John Wiley and Sons, Inc., New York, 1969, pp. 361-380.

[7] Nagaraja, K. S., "Analytical and Experimental Aeroelastic Studies of a Helicopter Rotor in Vertical Flight," Ph.D. Thesis, School of Aerospace Engineering, Georgia Institute of Technology, Atlanta, Georgia, 1975.

[8] Pierce, G. A. and White, W. F., "Unsteady Rotor Aerodynamics at Low Inflow and Its Effect on Flutter," AIAA Paper 72-959, Palo Alto, Calif., 1972.

Airfoil Design by Optimization

P. Ramamoorthy*
National Aeronautical Laboratory, Bangalore, India
and
K. Padmavathi†
Aeronautical Development Establishment, Bangalore, India

I. Introduction

THE inverse problem of determining an airfoil to support a given pressure distribution is an extremely important problem in aircraft design. This ensures the kind of flow that a designer wishes the wing to support so that criteria like shock delay and separation free zone are achieved at the design condition.

This problem has already been tackled by Lighthill[1] and Thwaites[2] in the forties by conformal transformation methods. In those days electronic digital computers were not available and emphasis was more and more on analytical methods which could not take care of all realistic situations adequately. The present method utilizes an analytical method for representing the airfoil contour by Wagner functions[3] and a computational procedure for obtaining the values of the coefficients of expansion. Lighthill's method could be applied only for a class of airfoils and Thwaite's method[2] is limited by convergence difficulties. The method given in this report is in that sense universal.

Section II gives the representation of an airfoil contour by Wagner functions. Section III validates the procedures for a NACA 0009 airfoil while in Sec. IV it is applied to a typical airfoil which gives a "roof-top" pressure distribution.

II. Representing an Airfoil Contour by Wagner Functions

In an earlier report[6] a procedure was given for approximating an airfoil contour by Wagner functions. Only a few details are given in this section. The slope of an airfoil can be approximated by a Fourier type of series of Wagner functions wherein the coefficients are determined by the method of least squares. Let $y=f(x)$ represent the airfoil contour. Then the slope $f'(x)$ is given by

$$f'(x)=\sum_{n=0}^{\infty} a_n h_n(x) - a_0 \tag{1}$$

where a_0 is the trailing-edge slope and $h_n(x)$ are called Wagner functions[3] defined by

$$h_n(x)=\frac{1}{\pi}\frac{T_{n+1}(1-2x)+T_n(1-2x)}{(x-x^2)^{1/2}} \qquad 0\le x\le 1 \tag{2}$$

Here $T_n(x)$ are Tychebychev polynomials. Putting

$$x=\sin^2\frac{\theta}{2}, \qquad 0\le\theta\le\pi \tag{3}$$

we have

$$h_n(\theta)=\frac{2}{\pi}\frac{\cos(\overline{n+1}\theta)+\cos\upsilon\theta}{\sin\theta} \tag{4}$$

First three Wagner functions are given by

$$h_0(\theta)=\frac{2}{\pi}\cot\frac{\theta}{2}$$

$$h_1(\theta)=\frac{2}{\pi}\left(\cot\frac{\theta}{2}-2\sin\theta\right)$$

$$h_2(\theta)=\frac{2}{\pi}\left(\cot\frac{\theta}{2}-2\sin\theta-2\sin 2\theta\right) \tag{5}$$

The recurrence relation satisfied by $h_n(x)$ is

$$h_n(n)=2(1-2x)h_{n-1}(x)-h_{n-2}(x) \tag{6}$$

Integrating Eq. (1) and changing the variables from x to θ, we get

$$f(x)\equiv z(\theta)=a_0\frac{(\theta+\sin\theta)}{\pi}+\frac{1}{\pi}\sum_{n=1}^{\infty}a_n\left(\frac{\sin\overline{n+1}\theta}{n+1}+\frac{\sin n\theta}{n}\right)$$
$$-a_0\sin^2\frac{\theta}{2} \tag{7}$$

Received July 26, 1976; revision received Sept. 28, 1976.
Index categories: Aircraft Configuration Design; Aircraft Aerodynamics.

*Scientist, Aerodynamics Division.
†Senior Scientific Officer.